Land Use Classification as a Key Component for Path Loss Prediction in Rural Areas

Melanie Neunerdt, Alexander Engels, and Rudolf Mathar
Institute for Theoretical Information Technology
RWTH Aachen University, Germany
{neunerdt,engels,mathar}@ti.rwth-aachen.de

***Abstract*—Path loss prediction is an essential building block for planning and optimization of cellular radio networks. Semi-empirical land use based models yield accurate and efficient path loss prediction results in rural areas. Consequently, land use information serves as a key input for those models. In this paper, we present a new $C \times K$-*Nearest-Mean* classification method operating on landscape images to provide the required input data for land use based path loss prediction models. With respect to this purpose our approach exceeds conventional land use classification using a neural network particularly in terms of total error rate. Utilization of our classification method by a specific path loss prediction model leads to prediction results with a mean square error of less than 6dB.**

I. Introduction

For effective planning and optimization of cellular radio networks path loss prediction is required, see [1]. Ray optical algorithms often achieve very high prediction accuracy, see [2], and are often used for path loss prediciton in urban areas. In rural areas, semi-empirical land use models yield accurate and efficient path loss prediction results. For instance, Erceg's widely-used path loss model [3] predicts path loss by choosing one fixed land use type for a considered prediciton area. In [4], a direction-specific land use based path loss model calculates path loss by considering the particular radio wave propagation characteristics of *all* land use segments that lay on the direct path between receiver and transmitter. A similar approach including different land use types is presented in [5].

However, all of these models need suitable land use information for the considered prediction area as input data. Since purchasing land use data is very expensive, we propose a new $C \times K$-*Nearest-Mean* classification method that operates on landscape images such as aerial photographs or satellite image data as a less expensive alternative. Particularly, our classification method provides the relevant land use input data demanded by DiLaP. General information on existing classification methods can be found in [6] and [7], respectively.

As cost-saving land use maps used for the classifier training process suffer from partially defective information, adequate handling of that property is a challenge for designing an appropriate classification method. In this paper, we develop a land use classification method that is robust against imbalanced and noisy training data. Adaption to a specific path loss prediction model leads to accurate path loss prediction results for rural areas.

The remainder of this paper is organized as follows. In Section II, we show how the prediction quality of the considered path loss model is related to the land use input data. Afterwards, we describe the data preprocessing in Section III and the new $C \times K$-*Nearest-Mean* classification method to generate the required land use information from landscape images in Section IV. In Section V, we validate the quality of our new classification method and compare it to a conventional neural network approach in terms of total error rate. Finally, in Section VI we conclude this paper.

II. Considered Path Loss Model

Common path loss prediction models such as Erceg's model and others, see [3], [8], define a distance dependent signal attenuation but leave alternating land use types between transmitter and receiver unconsidered. Thus, all receiver points at the same distance from the transmitter gain identical path losses. Obviously, this often does not correspond to reality. As illustrated in Figure 1, in a typical rural area, the two receivers $r1$ and $r2$ will experience different signal attenuation due to differing land use segments on their individual path to transmitter t, even if they are located at the same distance d from the transmitter. The ***Di**rection-specific **La**nd use based **P**ath loss model (DiLaP)* is intended for application in rural areas containing multiple land use types. Different land use types basically have different attenuation properties on the straight ray from receiver to transmitter. Accordingly, the model is not only restricted to one land use type but considers all land use segments - with varying sizes and types - that are passed by the straight way from receiver to transmitter. Moreover, smart direction-specific evaluation from receiver to transmitter is realized, which causes a stronger influence of land use segments that are located nearby the receiver as compared to the segments further away. This approaches a more realistic outcome.

For the path loss prediction, the model considers all $i = 1, \ldots, n(r)$ segments of conjoined differing land use classes $c(i) \in \mathcal{C} = \{FS \text{ (free space)}, VL \text{ (village)}, FR \text{ (forest)}\}$ on the direct path from receiver r to transmitter t according to

$$\begin{aligned} L^{\text{dB}}_{\text{DiLaP}}(r) &= C_f + \gamma_{c(1)}\, 10 \log_{10}\left(d(1)\right) \\ &+ \sum_{i=2}^{n(r)} \gamma_{c(i)}\, 10 \log_{10}\left(1 + \frac{d(i)}{\sum_{j=1}^{i-1} d(j)}\right) \end{aligned} \quad (1)$$

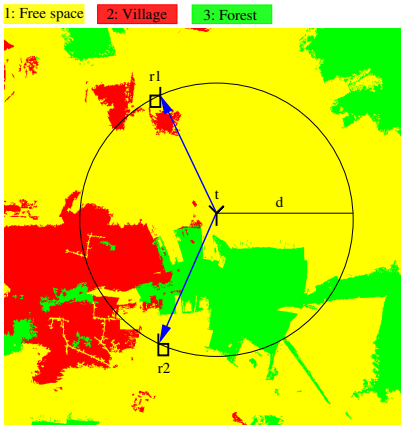

Fig. 1. Rural area containing three land use classes.

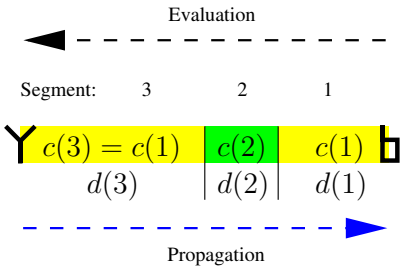

Fig. 2. DiLaP path evaluation principle.

where $d(i)$ denotes the length of segment i, $c(i)$ its land use class, $\gamma_{c(i)}$ the path loss coefficient, and the parameter C_f is an offset and frequency dependent parameter. Figure 2 depicts the idea behind formula (1), particularly the logical evaluation direction that is reverse to the physical propagation direction. For example, path loss contribution of segment 2 is calculated as the path loss with respect to the corresponding land use class $c(2)$ and distance ratio $(d(1) + d(2))/d(1)$. Obviously, DiLaP prediction quality and computational effiency strongly depends on the number and correctness of the evaluated land use segments. Therefore, application of the described path loss model requires knowledge of the land use class for each pixel in the considered area and the corresponding land use segment. For the considered set $\mathcal{C}$ of land use classes this leads to a three-class classification problem.

III. Data Preprocessing and Feature Extraction

Generally, a sufficient amount of training data serves as input for calibrating a classifier. For training purposes we use eleven sets of 1000×1000 pixel landscape images and corresponding pre-classified landuse maps with a resolution of $6.25m^2$ per pixel. We use cost-saving aerial photographs as landscape images.

Furthermore, the preprocessing of the landscape images is separated from the preprocessing of the corresponding land use maps. Preparation of the landscape images aims at providing suitable input data for the classification method, i.e., converting image information to an appropriate data representation. Particularly, we utilize an image segmentation technique for this task. The preprocessing of the land use maps includes the mapping from 24 existing land use classes to the three relevant classes $\mathcal{C} = \{FS, VL, FR\}$. The mapping process is not described in detail here. Table I describes the assignment from occurring landscape elements to the considered land use classes. As the land use maps suffer from partially defective land use information they can not be mapped precisely into these three classes. Hence, this leads to defective training data. Basically, image classification approaches can be devided into two categories based on the underlying image content representation. Approaches of the first category devide the image into principal components and use their characteristics for classification. Approaches of the second category classify by means of global features derived from the image as a whole. In this paper, we use an approach from the first category and treat image segments as principal components.

TABLE I
Definition of relevant land use classes.

Class	Landscape elements
Free space	location without vegetation, grassland, arable land, streets, tracks
Forest	coniferous forest, deciduous forest mixed forest
Village	buildings, vegetation inside of residential areas, front gardens

A region growing method, see [9], is used to extract regionally connected homogeneous landscape segments from the image. Here, the inital seed pixel for the region growing method is chosen randomly. Starting with the seed pixel the region grows to adjacent neighbouring pixels depending on a similarity criterion. We define the similarity criterion as the Euclidean distance compared to a threshold D, i.e.,

$$\sqrt{(\bar{x}_R - y_R)^2 + (\bar{x}_G - y_G)^2 + (\bar{x}_B - y_B)^2} < D \ , \qquad (2)$$

where $\boldsymbol{x} = (\bar{x}_R, \bar{x}_G, \bar{x}_B)$ is the mean RGB vector of the region up to the present state and $\boldsymbol{y} = (y_R, y_G, y_B) \in \{0, \ldots, 255\}^3$ is the the RGB vector of the considered adjacent neighbour pixel. The neighbour pixel $\boldsymbol{y}$ is added to the region if inequality (2) is fulfilled. We define the pixel neighborhood as the four horizontally and vertically connected pixels. The region growing process stops when all image pixels are assigned to a region. Each obtained region represents a segment for further processing.

We apply a feature analysis to derive the describing feature vector $\boldsymbol{x}$ for each image segment. In doing so, we analyse color, texture, form and size. To identify suitable features for differentiating between the three relevant land use classes, we perform extensive measurements and comparisons between segment features of different classes. This leads to five features that represent an image segment suitably: The mean RGB vector $\boldsymbol{x}_{RGB}$, homogeneity x_H and contrast x_C from the Haralick'sche texture parameters [10],the number of pixel x_S (size), the ratio x_P between the segment size and finally

the size of the minimal circular enclosure area. Therefore, in the classification process a segment SE is represented by its feature vector $\boldsymbol{x}_{SE}$ with the components

$$(\boldsymbol{x}_{RGB}, x_H, x_C, x_S, x_P) \in [0,1]^3 \times [0,1] \times \mathbb{R} \times \mathbb{R} \times [0,1] \ .$$

Consequently, the training data is represented by N training data sets $\{(\boldsymbol{x}_i, c_i)|i = 1 \ldots N\}$ with feature vectors $\boldsymbol{x}_i$ and the corresponding class labels c_i.

IV. $C \times K$-Nearest-Mean Classification

Developing a classifier typically consists of a training phase, where the classifier is trained to separate the various classes of objects based on the training data sets, and the application phase where the unknown class for considered objects is determined. However, we combine both of these phases and develop the classification rules directly while operating on the bare training data.

A. The algorithm

We introduce the $C \times K$-*Nearest-Mean Method* as a modified version of the *K-Nearest Neighbour Method (KNN)* [11] for image segment classification considering C relevant classes. An important benefit is the effective handling of defective training data. As described in Algorithm 1, our approach determines the unknown land use class for a segment SE represented by its feature vector $\boldsymbol{x}_{SE}$. The classification decision basically relies on the distances between $\boldsymbol{x}_{SE}$ and all feature vectors from training data $T = \{(\boldsymbol{x}_i, c_i)|i = 1 \ldots N\}$ with $c_i \in \mathcal{C} = \{FS, VL, FR\}$, i.e., $C = |\mathcal{C}| = 3$.

In contrast to the KNN method – where the classification rule is based on the K nearest neighbours over *all* training data sets – we determine the K nearest neighbours of *each* class in $\mathcal{C}$. Furthermore, our classification rule uses K *distances* of the nearest neighbours and, hence, CK distances are taken into account. In step 1 of Algorithm 1, the distances are calculated and sorted ascendingly for each class separately. Since the amount of training data sets is imbalanced for the three classes, in step 2 the successive mean of the $k = 1, \ldots, K$ nearest training data sets is calculated for each class. The scoring step 3 works as follows. For each position $k = 1, \ldots, K$ the class with the minimum successive mean value scores a one whereas the others do not score. To consider the imbalanced amount of training data sets appropriately, the scores are adapted by multiplication with a ratio factor. Finally, based on the total scores over all K positions, segment x_{SE} is assigned to the class with the maximum score. The classification process stops when all image segments are classified according to Algorithm 1.

We define the distance measured between two feature vectors $\boldsymbol{x}$ and $\boldsymbol{y}$ as distance function

$$\begin{aligned} d(\boldsymbol{x}, \boldsymbol{y}) &= w_1 \cdot ||\boldsymbol{x}_{RGB} - \boldsymbol{y}_{RGB}||_2 + w_2 \cdot |x_H - y_H| \\ &+ w_3 \cdot \frac{|x_K - y_K|}{\max(x_K, y_K)} + w_4 \cdot \frac{|x_S - y_S|}{\max(x_S, y_S)} \\ &+ w_5 \cdot |x_P - y_P| \end{aligned}$$

with feature weights $w_1, \ldots, w_5 \in \mathbb{R}$.

Algorithm 1 $C \times K$-Nearest-Mean

Input: Segment $\boldsymbol{x}_{SE} = (\boldsymbol{x}_{RGB}, x_H, x_P, x_S, x_C)$, training data T, parameter K, set of land use classes $\mathcal{C} = \{FS, VL, FR\}$

1: For all N_c elements of each class $c \in \mathcal{C}$ compute the distance d^c to $\boldsymbol{x}_{SE}$ and sort the distances ascendingly:

$$d^c_{min_1}, d^c_{min_2}, \ldots, d^c_{min_{N_c}}$$

2: For the first $K \leq N_c$ distances of each class $c \in \mathcal{C}$ compute the successive mean values:

$$d^c_{s_1}, d^c_{s_2}, \ldots, d^c_{s_K} \ , \quad d^c_{s_i} = \frac{1}{i} \sum_{j=1}^{i} d^c_{min_j}$$

3: For each position $1 \leq k \leq K$ score each class $c \in \mathcal{C}$ by

$$P\left(c, d^{FS}_{s_k}, d^{VL}_{s_k}, d^{FR}_{s_k}\right) = \begin{cases} 1 & d^c_s = \min\left\{d^{FS}_{s_k}, d^{VL}_{s_k}, d^{FR}_{s_k}\right\} \\ 0 & \text{otherwise} \end{cases}$$

4: Sum up the scores for each class $c \in \{FS, VL, FR\}$:

$$sum_c = \left[\sum_{k=1}^{K} P\left(c, d^{FS}_{s_i}, d^{VL}_{s_i}, d^{FR}_{s_i}\right)\right] \frac{\max(N_{FS}, N_{VL}, N_{FR})}{N_c}$$

Output: $c_{SE} = \underset{c \in \{FS,VL,FR\}}{\operatorname{argmax}} (sum_c)$

TABLE II
Feature weights.

Weight	w_1	w_2	w_3	w_4	w_5
Value	0.18	0.10	0.17	0.25	0.17

Comprehensive evaluation, aimed at satisfying parameter constellations, leads to the feature weights listed in Table II for $K = 80$ considered neighbours.

B. Classification postprocessing (smoothing)

As the classification results obtained by our $C \times K$-Nearest-Mean method serve as input data for the DiLaP path loss prediction model and because the computational efficiency of DiLaP is highly swayed by the number of land use segments, the postprocessing step serves to reduce the number of land use segments to a moderate amount. Due to the minor effect of small vegetation areas within residental areas to radio wave propagation, such areas are assigned to the land use class VL (village). This allows us to obtain large connected areas which contain fewer land segments for consideration in path loss prediction.

The postprocessing is realized in two successive smoothing steps which are applied to the classified image. In the first smoothing step, we identify the dominating class c_{MAX} within a virtual window area disjunctly slided through the image. For each $150m \times 150m$ virtual window we count the number

(a) Test image 7.

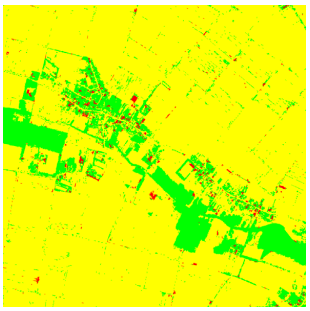

(b) Classification result.

Fig. 3. Test image classification, source: © LVA NRW.

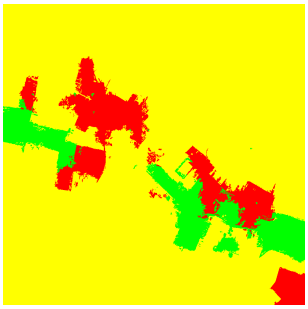

(a) Smoothing result.

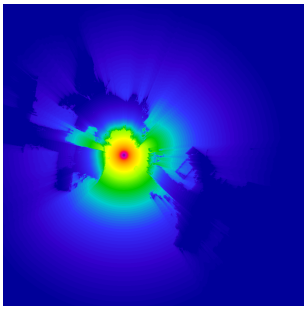

(b) DiLaP prediction.

Fig. 4. Exemplary land use based path loss prediction.

of pixels N_{FS}, N_{VL}, N_{FR} for the land use classes. The dominating class c_{MAX} is calculated as

$$c_{MAX} = \underset{c \in \{FS,VL,FR\}}{\operatorname{argmax}} \; (g_c N_c) \; . \tag{3}$$

for class-specific weight factors $0 \leq g_{FS}, g_{VL}, g_{FR} \leq 1$. All segments that lay within the window area with more than 50% are assigned to class c_{MAX} if

$$g_{c_{MAX}} N_{c_{MAX}} > 0.5 \; .$$

The second step is performed to analogously slided virtual windows of $100m \times 100m$. Again, we count the pixel numbers N_{FS}, N_{VL}, N_{FR} and determine c_{MAX} and $N_{c_{MAX}}$. We assign all segments covered with more than 50% and with a size below 20 pixel to the class c_{MAX} given by (3) using $g_c = 1$ for all $c \in \mathcal{C}$.

Applying the smoothing steps to the classification results provides suitable input data for DiLaP. Figure 3 illustrates the classification results for an exemplary training data landscape image depicted in Figure 3(a), where green color indicates forest, yellow color represents free space and village is colored red. For the proposed segment based $C \times K$*-Nearest-Mean* method the location of vegetation is not taken into account. According to the training data, with the exception to forest and tree groves which are also classified as forest, all vegetation is classified as free space. Figure 4(a) demonstrates the result of the two smoothing steps applied to Figure 3(b). Utilizing this as input data for DiLaP leads to the path loss prediction depicted in Figure 4(b).

It is important to notice that the sliding window sizes have to be chosen carefully. Improper sizing can lead to undue remerging of successfully separated land use segments in oversized windows and to insufficient smoothing for keeping the path loss calculation complexity low in window sizes that are to small.

V. Method Evaluation

The Cross validation technique is a common method for evaluation of classification performance, see [12]. The idea is to partition the training data into m complementary subsets, to perform the training on $m-1$ subsets (training data), and to validate the classification results with respect to the remaining subset (test set). This is repeated m-times such that each subset is used once as validation set. Here, we use $m = 11$ aerial photographs as complementary subsets and perform the $C \times K$*-Nearest-Mean* classification for each aerial photograph. The classification error rates are calculated by considering all image pixels. As shown in Table III, applying our proposed method we achieve cross validation error rates between 1% and 20% for the given training images.

We compare our classification results to those obtained by using a neural network as a widely-used conventional classifier, see [6]. The most significant advantage of neural networks is their generality which allows for application without having detailed information about the data being classified. A significant drawback of neural networks is the intransparent classification rule and the inability to apply selective modifications. Therefore, counteracting against effects of defective training data is not possible in the way our $C \times K$*-Nearest-Mean* classification approach allows for. We do not discuss the neural network structure in detail here and instead focus on the cross validation error rates compared to our method.

Counteracting the imbalanced and partially defective training data by choosing appropriate classification parameters K and $w_1, \ldots, w_5$ leads to the error rate comparison shown in Table III. By applying the smoothing operations to both classification methods our approach achieves mean error rates of 9% which exceeds the quality of the neural network results significantly.

Furthermore, we consider classification accuracy for the single classes by means of evaluating the confusion matrix, see [13]. The confusion matrix shows the relative frequencies of predicted class relative to the true class accumulated over all image pixels. The results for the exemplary image from Figure 3(a) are listed in Table IV. Particularly recognition rates for the land use classes FS (free space) and FR (forest) are important for classification in rural areas that are typically dominated by free space and forest areas. As our proposed method allows for selective parameter adaption, free space and forest are recognized successfully by $C \times K$*-Nearest-Mean* classification with 91% and 95%, respectively, see diagonal entries of the upper confusion matrix entries in Table IV.

Postprocessing, i.e., smoothing, is applied to the exemplary classification results and particularly enhances classification

TABLE III
ERROR RATES ACCORDING TO CLASSIFICATION WITH SMOOTHING

Test Image	**Neural Network**	$C \times K$**-Nearest-Mean**
1	55%	20%
2	25%	10%
3	5%	15%
4	40%	8%
5	4%	4%
6	64%	11%
7	5%	4%
8	18%	1%
9	29%	14%
10	8%	5%
11	12%	2%
Mean value	24%	9%

TABLE IV
CLASSIFICATION RESULTS IN FORM OF CONFUSION MATRICES.

True/ Predicted	**village**	**free space**	**forest**
A: $C \times K$**-Nearest-Mean**			
village	16%	1%	1%
free space	23%	91%	4%
forest	61%	8%	95%
B: $C \times K$**-Nearest-Mean with Smoothing**			
village	80%	3%	1%
free space	13%	97%	0%
forest	7%	0%	99%
B-A: Absolute differences			
village	+64%	+2%	0%
free space	−10%	+6%	−4%
forest	−54%	−8%	+4%

of the land use class village, see the entries of the second confusion matrix in Table IV. This effect becomes obvious when comparing the elementwise absolute differences of the confusion matrix entries corresponding to classification with and without smoothing, see lower part of Table IV.

VI. CONCLUSIONS

In this work, we present a new $C \times K$*-Nearest-Mean* classification method to provide input data for land use based path loss prediciton models. We adapt our classifiction algorithm particularly for the DiLaP path loss prediction model. Concerning a considerable amount of test data, we achieve a mean classification error rate of 9% which exceeds the error rate quality obtained by conventional neural network classification significantly.

Utilizing our approach to generate input data for DiLaP path loss prediction leads to prediction results with mean square errors of less than 6dB. Particularly, this demonstrates that the combination of appropriate land use classification and an accurate path loss prediction model allows for yielding excellent radio wave prediction results in rural areas.

VII. ACKNOWLEDGMENT

This work was partially supported by *UMIC*, a research project in the framework of the German excellence initiative, and the *Project House HumTec* at RWTH Aachen University, Germany.

REFERENCES

[1] E. Amaldi, A. Capone, and F. Malucelli, "Radio planning and coverage optimization of 3g cellular networks," *Wirel. Netw.*, vol. 14, no. 4, pp. 435–447, 2008.
[2] R. Mathar, M. Reyer, and M. Schmeink, "A cube oriented ray launching algorithm for 3D urban field strength prediction," in *IEEE ICC 2007*, Glasgow, Jun. 2007.
[3] V. Erceg, L. Greenstein, S. Tjandra, S. Parkoff, A. Gupta, B. Kulic, A. Julius, and R. Bianchi, "An empirically based path loss model for wireless channels in suburban environments," *Selected Areas in Communications, IEEE Journal on*, vol. 17, no. 7, pp. 1205–1211, Jul 1999.
[4] A. Engels, M. Reyer, and R. Mathar, "A Direction-Specific Land Use Based Path Loss Model for Suburban/Rural Areas," *IEEE Symposium on Anntenas and Propagation*, Jul 2010.
[5] M. Döttling and W. Wiesbeck, "A hierarchical electromagnetic land use parameter data base for wave propagation modeling," Institut für Höchstfrequenztechnik und Elektronik, Tech. Rep., 2008.
[6] C. M. Bishop, *Pattern recognition and machine learning*. New York: Springer, 2006.
[7] R. O. Duda, P. E. Hart, and D. G. Stork, *Pattern Classification*, 2nd ed. New York: Wiley-Interscience, 2001.
[8] V. S. Abhayawardhana, I. J. Wassell, D. Crosby, M. P. Sellars, and M. G. Brown, "Comparison of empirical propagation path loss models for fixed wireless access systems," in *Vehicular Technology Conference, 2005. VTC 2005-Spring. 2005 IEEE 61st*, vol. 1, 2005, pp. 73–77 Vol. 1.
[9] R. C. Gonzalez and R. E. Woods, *Digital Image Processing*, 2nd ed. Addison-Wesley Publishing Company, 2002.
[10] R. Haralick, K. Shanmugam, and I. Dinstein, "Textural features for image classification," *Systems, Man and Cybernetics, IEEE Transactions on*, vol. 3, no. 6, pp. 610–621, 1979.
[11] T. Cover and P. Hart, "Nearest neighbor pattern classification," *Information Theory, IEEE Transactions on*, vol. 13, no. 1, pp. 21–27, 1967.
[12] P. Devijver and J. Kittler, *Pattern recognition: A statistical approach*. Prentice Hall, 1982.
[13] F. Provost, *Machine Learning*. Springer US, 1998.